ACS OMEGA

Open Access

http://pubs.acs.org/journal/acsodf

Article

Long-Term Antioxidant Metal−Organic Frameworks

Woojin Park, Sanghyun Park, Ki-Youb Park, and Eun-Young Choi*

Cite This: *ACS Omega* 2024, 9, 21484−21493

Read Online

ACCESS | Metrics & More | Article Recommendations | Supporting Information

ABSTRACT: Free radicals produced during metabolism induce effects, such as cell damage and cancer, because of their high reactivity. Although antioxidants in food products can eliminate free radicals, they are expelled within a relatively short period of time after serving their function. In this study, we investigated the possibility of using metal−organic frameworks (MOFs) with antioxidants as their ligands. Metal−organic frameworks are crystalline polymers with repetitively coordinated ligands and metal centers. We assume that once antioxidant-based MOFs are ingested, ligands are released on a long-term basis during the process of chemical and physical disintegration. To evaluate their eligibility, we established criteria for biocompatibility, particle size, and long-term antioxidant effects. For biocompatibility, we treated cells with various concentrations of MOFs and their precursors followed by a water-soluble tetrazolium 8 (WST-8) assay. The particle size distribution was analyzed using TEM and ImageJ software, and the antioxidant release was quantified using UV−vis spectroscopy. We concluded that Fe-based FeTHQ with the antioxidant tetrahydroxy-1,4-benzoquinone (THQ) as its ligand is the most effective long-term antioxidant with its effect lasting up to 7 days. Furthermore, microwave synthesis of FeTHQ was conducted to produce more suitable particles for *in vivo* antioxidant applications.

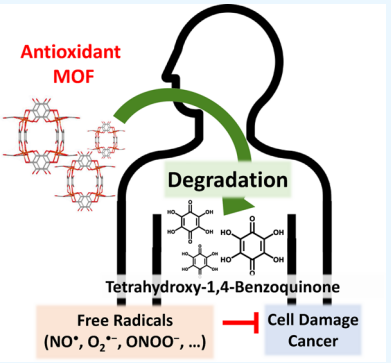

1. INTRODUCTION

Antioxidants play an essential role in cellular health by removing free radicals created during metabolic processes. Although cells have a built-in mechanism of free radical removal, such as the enzyme superoxide dismutase, it is not sufficient to fully protect the cell from damage. Therefore, antioxidants must be ingested for optimal health.[1] Despite the well-documented benefits of antioxidants, their effective delivery and long-term retention in the body pose significant challenges. The rapid metabolism and excretion of antioxidants limit their potential to counteract oxidative stress over extended periods. This limitation underscores the need for innovative strategies to enhance the bioavailability and persistence of antioxidants within the body. Metal−organic frameworks (MOFs), because of their unique structural features and chemical versatility, offer a promising platform for addressing these challenges.

Metal−organic frameworks (MOFs), characterized by their crystalline porous structure composed of metal ions coordinated to organic ligands,[2] have emerged as a novel class of materials with diverse applications, including gas storage, separation, and catalysis.[3] In the field of biomedicine, MOFs have shown potential for drug delivery, thereby highlighting their ability to encapsulate bioactive molecules within their pores or release bioactive ligands through structural degradation. Both methods have been used in previous studies of antioxidant MOF research. Antioxidant and anticancer molecule doxorubicin was loaded inside Zr-MOF, and radical scavenging capabilities were measured without relation to time.[4] In another study, gallic acid, an antioxidant, was used as a ligand for MOFs and its ROS (reactive oxygen species) concentration was measured over 24 h.[5] However, no study has been conducted on the long-term antioxidant effects of MOFs. MOFs incorporate the antioxidant ligands into a bulky crystal, which leads to longer circulation time compared with single ligands and slow, controlled release of antioxidants. This study leverages the versatility of MOFs to explore their capacity as carriers of antioxidants and aims to provide a sustained antioxidant effect that overcomes the limitations of conventional antioxidant supplementation.

Given the potential adverse effects associated with some antioxidant compounds, such as the strong odor of thiols, this research focuses on catechol ligands for their favorable properties (Figure 1). Catechol, classified as phenol, is a generic term for benzene structures with two hydroxyl groups attached at the ortho position. The antioxidant properties of catechol are realized through the removal of hydrogen from the hydroxyl group. This study aims to synthesize catechol-based MOFs and evaluate their antioxidant efficiency, biocompatibility, and particle size distribution to ensure optimal absorption and circulation within the body.

Received: February 29, 2024
Revised: April 12, 2024
Accepted: April 19, 2024
Published: April 29, 2024

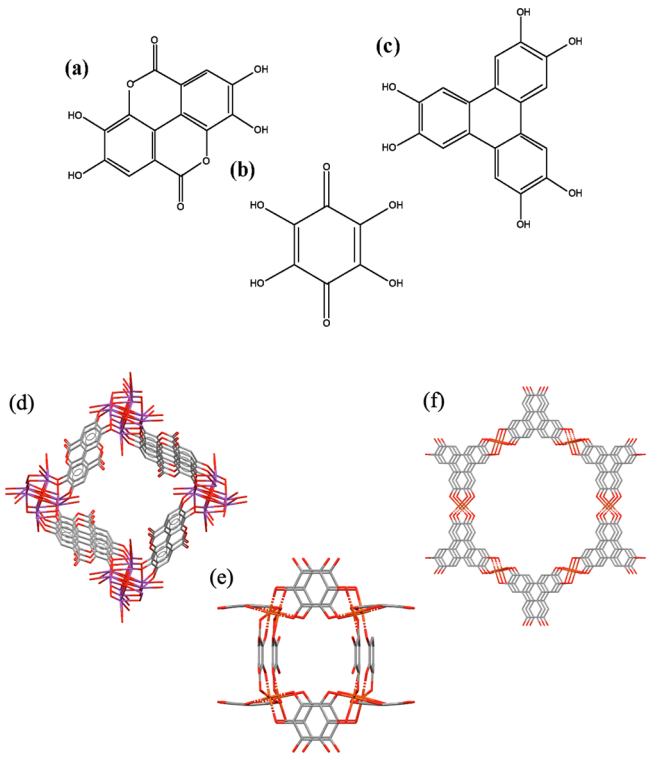

Figure 1. Ligand candidates and their respective MOFs. (a) Ellagic acid, (b) THQ, (c) HHTP, (d) SU-101 [$(C_{14}H_6Bi_2O_{11})_n{\cdot}2(H_2O)$, CCDC ref. code: DUVNOA], (e) FeTHQ [$(C_{18}Fe_4O_{18})_n{\cdot}6(H_2O)$, CCDC ref. code: QAMDOB], and (f) Cu-CAT-1 [$Cu_3(C_{18}H_6O_6)_2$, CIF file obtained from Zenodo[6]]. By investigating ligands that take the form of catechols in the Cambridge Structural Database,[7] 2199 candidates were derived. Considering the rigidity and symmetry of the ligands, ellagic acid, THQ, and HHTP were selected to determine whether they could act as MOF linkers. Considering the toxicity of metal ions,[8] bismuth-based SU-101, iron-based FeTHQ, and copper-based Cu-CAT-1 MOFs were selected.

2. EXPERIMENTAL SECTION

2.1. Chemicals. $Bi(OAc)_3$, $FeSO_4{\cdot}7H_2O$, $KMnO_4$, trolox, copper(II) trifluoroacetylacetonate, *N*-methyl-2-pyrrolidone (DMF), dimethylformamide (DMF), HCl, and acetic acid were purchased from Sigma-Aldrich. 2,2′-Azino-bis(3-ethylbenzothiazoline-6-sulfonic acid) (ABTS), ellagic acid, tetrahydroxy-1,4-benzoquinone (THQ), and 2,3,6,7,10,11-hexahydroxytriphenylene (HHTP) were obtained from TCI Chemicals. Ethyl alcohol (EtOH) was purchased from SAMCHUN Chemical.

2.2. MOF Synthesis. The MOFs were synthesized by using the following methods. For SU-101 (CCDC ref. code: DUVNOA), 0.15 g of ellagic acid and 0.38 g of $Bi(OAc)_3$ were added to a 6% acetic acid solution and stirred at rt for 48 h.[9] For FeTHQ (CCDC ref. code: QAMDOB), 0.03 g of THQ was dissolved in a solution consisting of 5 mL of DMF and 5 mL of H_2O, whereas 0.0969 g of $FeSO_4{\cdot}7H_2O$ was dissolved in 10 mL of H_2O. The two solutions were combined in a 20 mL scintillation vial, sonicated, and then kept in an oven (DKN 302 Oven) at 80 °C for 12 h.[10] Cu-CAT-1 (CIF file obtained from Zenodo[6]) was synthesized using a slightly modified solvothermal method.[11] A 0.0750 g amount of HHTP and 0.1050 g of copper(II) trifluoroacetylacetonate were dissolved in 10 mL of H_2O. NMP (1 mL) was added to this solution. The reaction mixture was heated in an oven at 85 °C for 12 h.

Additional synthesis of FeTHQ was attempted under various conditions in order to optimize the particle size. Solvothermal method was carried out with different synthesis time conditions of 1, 3, 6, and 12 h. Microwave synthesis (Discover SP Microwave, CEM Corporation) was also conducted because they are known for yielding smaller crystals because of the promotion of fast nucleation, therefore satisfying our purpose.[12] Solutions of 5 mL of THQ and $FeSO_4{\cdot}7H_2O$ with the same concentration as that used in the solvothermal method were pipetted into a 40 mL microwave reaction vessel and gently mixed through shaking. Fixed power method was used with a total of 18 combinations of varying time and power conditions.

After synthesis, the products were centrifuged at 4000 rpm for 10 min, and the supernatant was discarded. Solvent exchange was performed once in H_2O and twice in EtOH through vortexing. The powder was then dried in a 60 °C vacuum oven for 3 h, which resulted in activation.

2.3. MOF Characterization. The structures of the synthesized MOFs were elucidated by using X-ray diffraction (Rigaku MiniFlex 600) and IR spectroscopy (PerkinElmer Frontier FT-NIR). The particle size and morphology of each MOF were observed by using SEM (Zeiss GeminiSEM 500). In order to further characterize the microwave-synthesized FeTHQ, TGA (Scinco) and SEM (TESCAN S8000) analyses were additionally conducted. PXRD results of the TGA remnants were also investigated.

2.4. *In Vitro* Biocompatibility Test. The cytotoxic activities of the synthesized MOFs and their precursors were analyzed by using a WST-8 assay. Neural stem cells collected from the subventricular zone of mice were cultivated in 96-well plates supplemented with the N5 medium. Particle suspensions were prepared as a dilution series in N5 medium from 1 to 10 μg/mL. After treatment, the medium was replaced with the original N5 medium, and the cells were further incubated for 24 h in 5% CO_2 and 37 °C condition (Forma Series II water-jacketed CO_2 incubator). The cytotoxicity was determined by adding WST-8 reactant. A VersaMax microplate reader was used for quantitative analysis of the cell viability. WST-8 Cell Viability Assay Kit was purchased from Quanti-Max, and N5 medium was prepared in advance according to a previous report.[13] Phosphate-buffered saline (PBS) was purchased from GenDEPOT.

For the long-term biocompatibility test, we used Caco2 cells (purchased from Korean Cell Line Bank), which are human epithelial cells originated from the colon and commonly used as model cells for human small intestinal enterocytes. The frozen cell stock was thawed and directly plated in 96-well plates. The next day, the medium was replaced with fresh medium containing particles from 1 to 62 μg/mL with serial dilution. WST-8 cell viability test was performed after 6 days of incubation in particle containing medium. Culture medium was Dulbecco's Modified Eagle Medium supplemented with 10% fetal bovine serum (GenDEPOT), and penicillin/streptomycin (Sigma).

2.5. Antioxidant Capability Analysis. In order to mimic the intake pathway of the particles when ingested, 0.1 g of each MOF powder was stirred in HCl(aq) set to pH 2 for 2 h. Then, 1 mL of each of the solutions were collected in a 1.5 mL E-tube. Centrifugation was conducted to separate the MOF particles and supernatant. The remaining amount of the MOF

https://doi.org/10.1021/acsomega.4c01993
ACS Omega 2024, 9, 21484−21493

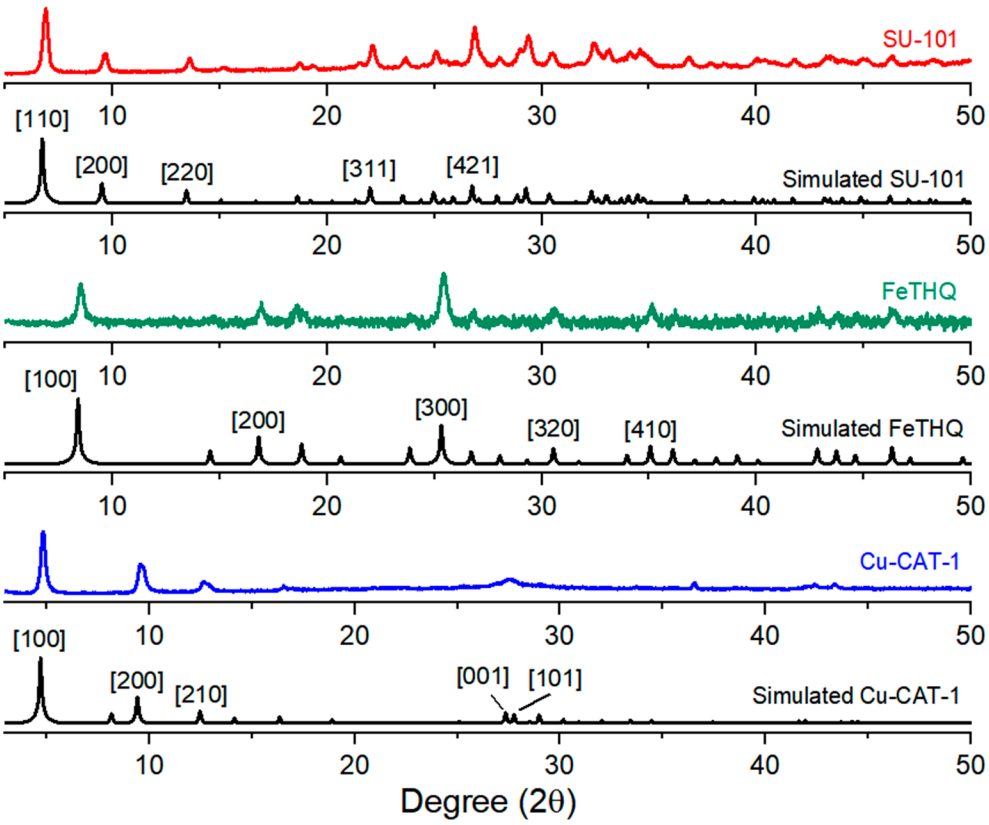

Figure 2. PXRD results of synthesized SU-101, FeTHQ, and Cu-CAT-1 and their simulated graphs

suspension was also centrifuged and activated to obtain pristine powders. The powder was then suspended in 30 mL of a PBS buffer and constantly stirred at 200 rpm. At every 12 h interval, 1 mL of the suspension was pipetted and then centrifuged to obtain the supernatant and powder. Particle size distribution analysis using TEM and antioxidant effect analysis with UV−vis spectroscopy (LAMBDA 365 UV−vis spectrophotometer) was performed to comprehensively evaluate each MOF's antioxidant capability.

2.5.1. Particle Size Analysis. The powders obtained during the initial pH 2 HCl suspension and each time interval in PBS were subjected to PXRD and TEM particle counting in order to qualitatively and quantitatively analyze the temporal change in particle size distribution. TEM analysis (Hitachi TEM H-7600) was performed on the powders and was combined with particle size counting using ImageJ software.[14] The size of 120 particles was measured from all samples.

2.5.2. Antioxidant Effect Quantitation. Oxygen radical absorbance capacity (ORAC) assay is a method for quantitatively measuring antioxidant activity with the dimension of μmol trolox g^{-1}, which indicates the effectiveness of the antioxidant compared with the vitamin-based antioxidant trolox. Alternatively, antioxidant activity can be measured through ABTS assay, which also uses trolox as a standard reference material with the final value represented as TEAC (trolox equivalent antioxidant capacity).[15] Therefore, we performed an ABTS assay to calculate the TEAC value and then converted it to the ORAC.

To quantify the antioxidant capacities of MOFs and their precursor ligands, ABTS standard solution was prepared according to prior research.[16] Standard solutions of ellagic acid, THQ, HHTP, and trolox were prepared and dissolved in EtOH. All solutions were diluted 2-, 4-, and 8-fold. Ten μL of each solution was mixed with 990 μL of ABTS standard in a plastic cuvette, and the absorbance at 734 nm was measured. All experiments were repeated three times to yield a calibration curve having % inhibition as the y axis. After calculating the IC_{50} value of the ligands and trolox, the TEAC value was calculated according to eq 1. Finally, the TEAC value was converted to the ORAC value according to eq 2.

$$\text{TEAC} = \frac{IC_{50}\ \text{of trolox}}{IC_{50}\ \text{of sample}} \tag{1}$$

$$\text{ORAC}(\mu\text{mol trolox g}^{-1}) = \frac{\text{TEAC}}{MW_{\text{trolox}}(250.29\ \text{g mol}^{-1})} \tag{2}$$

Calibration curves of standardized PBS solutions of ellagic acid, THQ, and HHTP were obtained through UV−vis analysis after selecting a representative peak (204, 319, and 274 nm, respectively, for ellagic acid, THQ, and HHTP in pH 2 HCl; 276, 363, and 274 nm, respectively, for ellagic acid, THQ, and HHTP in PBS). UV−vis analysis was performed on the supernatant samples collected during the intake mimicking suspensions. The absorbance values of the supernatants were fitted into their respective calibration curves to determine the amount of ligand expelled during each time period. The value was then normalized to the ligand production per unit mass of each MOF to yield the ORAC value of the MOFs.

2.6. Dynamic Light Scattering (DLS) Analysis. Both a 0.1 g amount of microwave-optimized FeTHQ and of solvothemally synthesized FeTHQ were each immersed in 30 mL of PBS buffer solution and stirred constantly at 200 rpm. Two mL samples were collected every 24 h for 7 days.

https://doi.org/10.1021/acsomega.4c01993
ACS Omega 2024, 9, 21484−21493

DLS analyzer (LS 13 320 particle size analyzer, Beckman Coulter) was used to observe temporal changes in the particle size distribution. We assumed that DLS analysis would yield distribution results that exhibit particle behavior in the suspension state.[17]

3. RESULTS AND DISCUSSION

3.1. MOF Synthesis. The synthesis of SU-101 resulted in the production of a yellow powder, whereas the synthesis of FeTHQ and Cu-CAT-1 resulted in black crystalline materials.

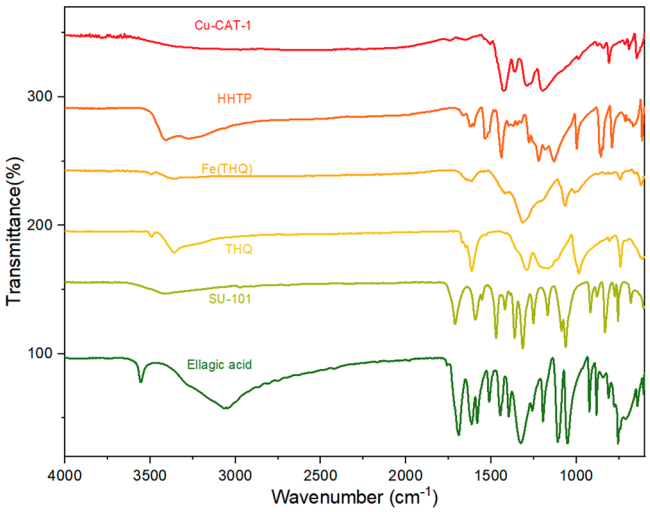

Figure 3. IR graphs of SU-101, FeTHQ, and Cu-CAT-1 and their catechol ligands ellagic acid, THQ, and HHTP.

3.2. MOF Characterization. The peaks derived from PXRD analysis matched those of the previously reported structures.[9−11] (Figure 2). IR analysis showed a decrease in the depth of the O−H stretch in the wavenumber range of 3000−3500 cm^{-1}, thereby proving the successful coordination of the metal ions and the deprotonated hydroxyl groups of each ligand (Figure 3). Rod-shaped crystals are observed in the SEM image of SU-101 (Figure 4a). FeTHQ had aggregated globular crystals, as shown in Figure 4b. Cu-CAT-1 showed thin planar crystals (Figure 4c).

3.3. *In Vitro* Biocompatibility Test. The biocompatibility of MOFs and their precursors is critical for antioxidant applications. The WST-8 assay showed that all substances, including metals, ligands, and MOFs, maintained over 100% viability at concentrations up to 10 μg/mL. Considering that cell viability is calculated by the ratio of absorbance, cases where the percentage exceeded 100% are valid to be considered as total survival. Therefore, SU-101, FeTHQ, and Cu-CAT-1 were safe for *in vivo* use at concentrations of less than 10 μg/mL (Figure 5).

In terms of long-term biocompatibility, the viability of Caco2 cells after 6 days of incubation with each of the MOFs is shown in Figure 6. Both SU-101 and FeTHQ demonstrated over 60% cell survival at concentrations up to 62 μg/mL. In contrast, the viability of Caco2 cells incubated with Cu-CAT-1 decreased progressively with increasing concentrations and reached as low as 13% at the highest concentration tested. As Mg-MOF-74, a MOF widely studied for drug delivery because of its biocompatible nature, resulted in having an IC_{50} value of 40 μg/mL in a previous study,[18] our result indicates that SU-101 and FeTHQ are feasible long-term antioxidants.

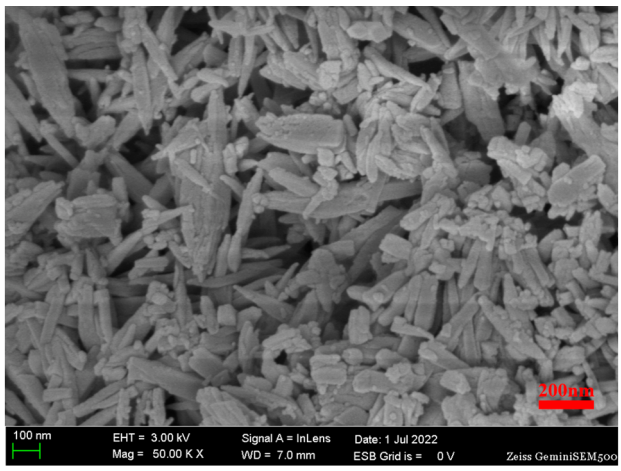

(a)

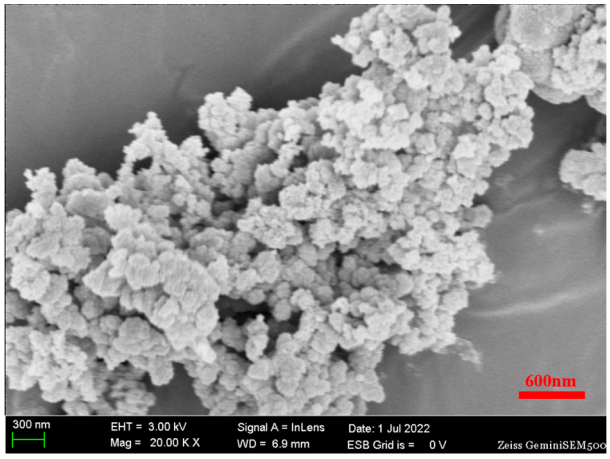

(b)

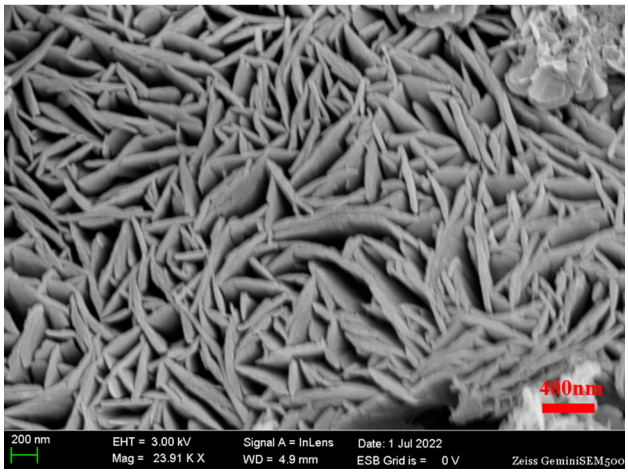

(c)

Figure 4. SEM image of synthesized MOFs: (a) SU-101, (b) FeTHQ, and (c) Cu-CAT-1.

3.4. Structural Degradation of FeTHQ Using PXRD. Structural degradation is necessary for the release of the antioxidant ligands. The PXRD results in Figure 8 show a gradual decrease in the main peaks of FeTHQ over time, which

https://doi.org/10.1021/acsomega.4c01993
ACS Omega 2024, 9, 21484−21493

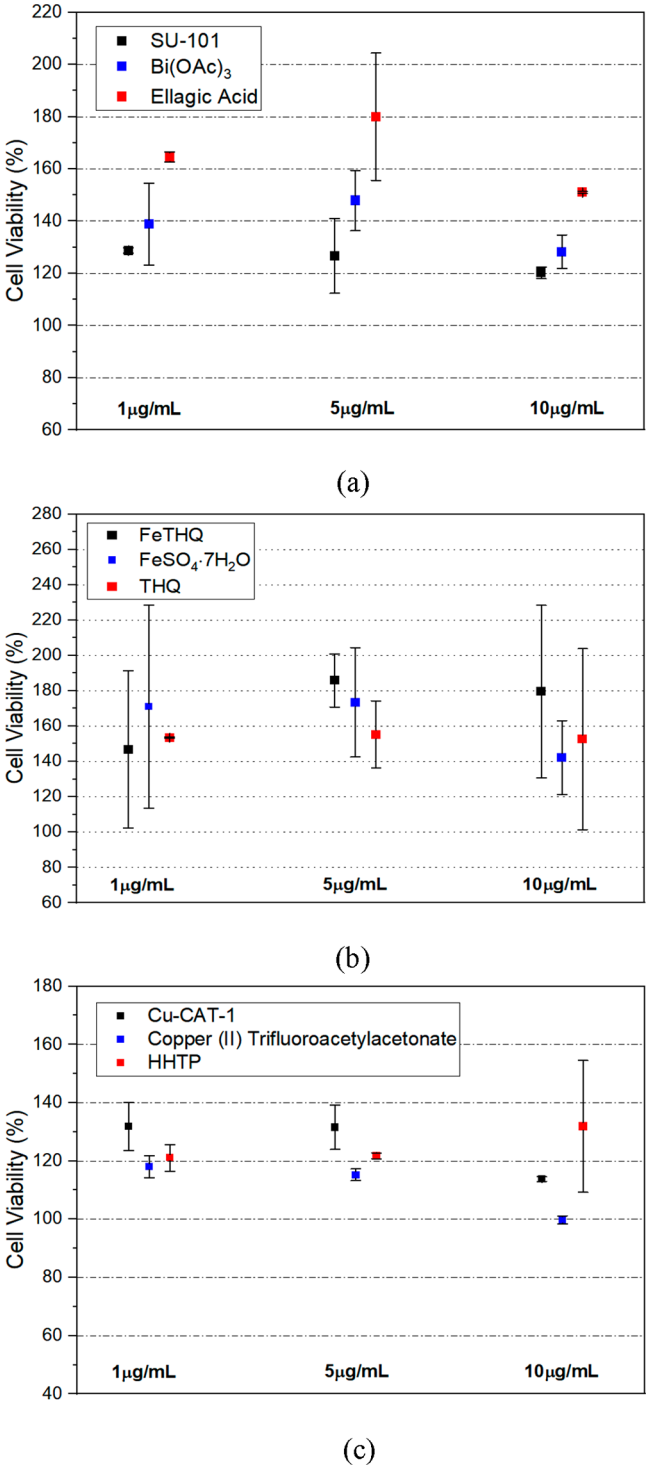

Figure 5. Cell viability results of MOFs and their precursors: (a) SU-101, (b) FeTHQ, and (c) Cu-CAT-1.

almost loses its main peaks after 200 h. Cu-CAT-1 also showed a decrease in the intensity of the main peaks, but the peaks were still visible after 200 h. SU-101 showed no significant decrease in the main peaks. Since degradation is proportional to antioxidant release, we can assume that antioxidant effect will take the sequence of FeTHQ > Cu-CAT-1 > SU-101.

3.5. ABTS Assay. The TEAC and ORAC values of each ligand are given in Table 1. These values are in agreement with the structures because HHTP has the most hydroxyl groups

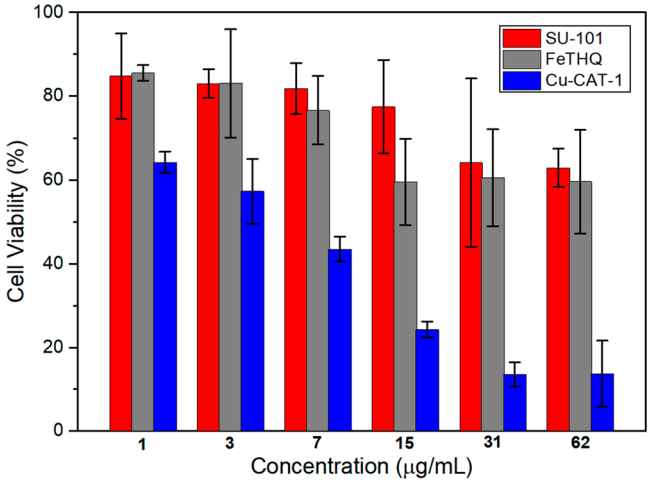

Figure 6. Long-term biocompatibility results of synthesized MOFs.

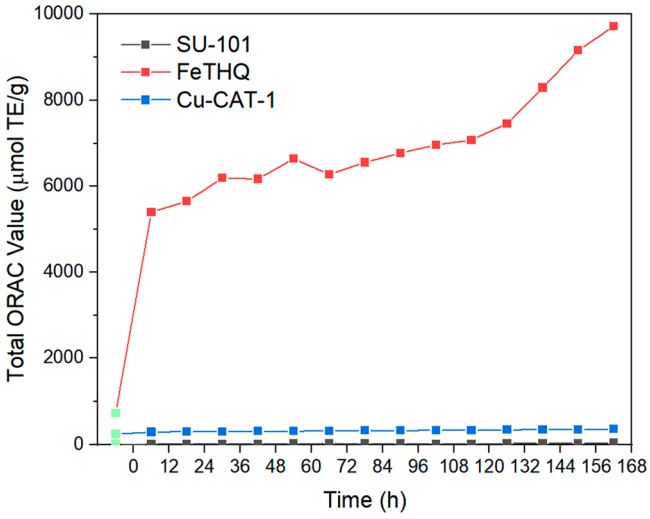

Figure 7. Comprehensive graph of 12 h interval of ORAC values of MOFs. The initial green dots stand for the ORAC values quantified when the MOFs were immersed in a pH 2 HCl solution for 2 h. The subsequent dots indicate instances when the MOFs were suspended in PBS solution.

with extended conjugation length, which remain stable even after deprotonation. Ellagic acid has less conjugation compared with HHTP, and THQ has the shortest conjugation length with one arene group.

3.6. Antioxidant Capability of MOFs. *3.6.1. Particle Size Distribution Analysis.* Particles between 0.1 and 100 μm in size, classified as microparticles (MPs), are absorbed in the small intestine and accumulate in the liver within 5 h after intake. MPs under 200 nm can pass through the liver and circulate in the blood until a gradual breakdown to the nanometer range enables filtration through the kidneys. Particles larger than 1000 nm are absorbed at a very low rate and mostly excreted.[19] Therefore, our goal is to synthesize a MOF between 200−1000 nm in size to ensure maximum absorption and circulation within the body.

The MOFs showed a decrease in the average particle size over time. SU-101 showed a significant reduction in particle size with most particles being less than 300 nm in size, as shown in Supplementary Figure 1b. FeTHQ showed a similar decreasing tendency, albeit not as significant as SU-101

https://doi.org/10.1021/acsomega.4c01993
ACS Omega 2024, 9, 21484−21493

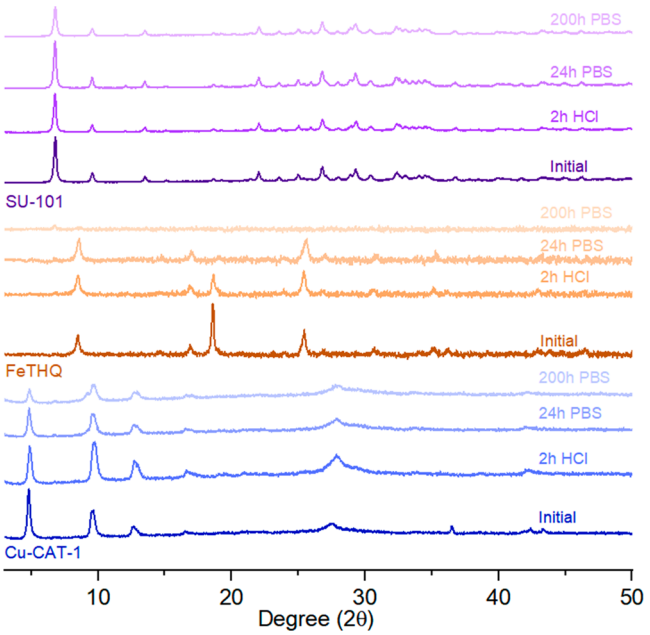

Figure 8. PXRD graphs of MOF in PBS and pH 2 HCl solution showing apparent structural degradation of FeTHQ compared with SU-101 and Cu-CAT-1.

Table 1. TEAC & ORAC Values of Antioxidant Ligands

	ellagic acid	THQ	HHTP
TEAC	2.03276	1.25473	4.03925
ORAC (μmol trolox g^{-1})	8121.6	5013.1	16138

(Supplementary Figure 1d). Cu-CAT-1 contained a considerable number of large particles compared with SU-101 and FeTHQ (Supplementary Figure 1f).

3.6.2. UV−Vis Quantification. For SU-101, less than 15 ORAC equivalents of ellagic acid were expelled during each 12 h interval (Supplementary Figure 2a). Considering that there are negative values of antioxidant production in some intervals resulting in an average of 2.4 mol % of the ORAC, we can assume that the release of ellagic acid from SU-101 is near 0.

In the case of FeTHQ, 4680 ORAC of THQ were emitted during the 0−12 h interval. After that, an average of 332 ORAC of ligand was constantly produced every 12 h. During the 2 h of FeTHQ in HCl, 727 ORAC of THQ were expelled (Supplementary Figure 2b).

For Cu-CAT-1, 247 ORAC equivalent of HHTP was released in the first 2 h in HCl, which was the highest amount in all time periods. On the basis of this result, we assumed that Cu-CAT-1 is unstable in an acidic environment. The material showed an average of 8 ORAC releases in the following intervals (Supplementary Figure 2c). The comprehensive results of the antioxidant effects shown in Figure 7 align with the predicted order in Figure 8.

3.7. Size-Optimal Synthesis of FeTHQ. Biocompatibility tests showed that all three MOFs were suitable for biological applications. Particle size distribution analysis determined that SU-101 and FeTHQ had optimal sizes for absorption in the body and an adequate circulation time. However, SU-101 did not exhibit a significant antioxidant activity. Therefore, FeTHQ was selected as the final candidate as a long-term antioxidant MOF. Subsequent experiments were conducted to optimize its particle size.

3.7.1. Solvothermal and Microwave Synthesis. Particle size distributions of synthesized FeTHQ are presented in Figure 9. Ironically, the solvothermal FeTHQs had smaller average particle sizes than the microwave FeTHQ series. In contrast, the microwave FeTHQs had a smaller proportion of crystals exceeding 1 μm in diameter and a narrower distribution in general.

The proportion of crystals less than 1 μm in diameter according to different synthesis procedures were measured (Supplementary Tables 1 and 2). For some of the microwave-assisted methods, the product yield was insufficient for particle size analysis. By selecting the combinations that resulted in more than 99% of crystals under 1 μm, a total of seven cases were chosen as FeTHQ candidates: 1 min at 100W, 10 min at 100 W, 30 s at 200 W, 30 s at 300 W, 1 min at 300 W, 5 min at 300 W, and 10 min at 300 W.

3.7.2. Characterization of FeTHQ Candidates. The PXRD results of the microwave FeTHQs generally had a much lower intensity than the solvothermally synthesized FeTHQ. This could be explained by the fact that MOF crystals have a shorter crystallization time when synthesized by using microwaves. However, the main peaks of the microwave series matched those of solvothermal FeTHQ (Supplementary Figure 3).

The IR results for the microwave series are shown in Supplementary Figure 4. We focused on the degree of lessening of the depth of the O−H stretch in the 3000−3500 cm^{-1} wavenumber range, which represents successful coordination between the deprotonated hydroxyl groups and metal ions. The 1 min at 300 W combination showed the greatest reduction in the depth of the O−H stretch compared with other methods. Considering the yield and PXRD intensity results, this combination was selected as the final candidate.

The SEM images of synthesized FeTHQ are shown in Figure 10. There is a clear particle size difference between the two synthesis methods, which conflicts with the previous particle size analysis results obtained using DLS in Figure 11. We suggest that agglomeration of microwave-synthesized FeTHQ occurs in suspension, which is explained in detail later. Microwave FeTHQ had a uniform particle size in contrast with the different sizes of solvothermal FeTHQ crystals.

The TGA curves of solvothermal FeTHQ and microwave FeTHQ showed similar tendencies (Supplementary Figure 5). Because the powder form size of the microwave FeTHQ particles is smaller, a larger surface area would be in contact with the heat source, thereby leading to accelerated degradation and weight loss. However, the final weight percentages of the two materials are almost the same (41.8% for solvothermal FeTHQ, 39.8% for microwave FeTHQ).

The PXRD peaks of both solvothermal FeTHQ and microwave FeTHQ remnants matched the simulated PXRD peaks of the Fd3m-type Fe_3O_4 (Supplementary Figure 6).

3.7.3. Particle Size Distribution of Microwave FeTHQ and Solvothermal FeTHQ. The particle size distribution of solvothermal FeTHQ shifted to the right when it was stirred in PBS, which indicated the presence of larger particles. Strangely, there was little or no tendency to decrease in the over time. In the case of microwave FeTHQ, each size distribution had a wider range compared with the previous dispositions even though the mode decreased continually. We assume that cations present in PBS, such as sodium and potassium, induce electrostatic screening, which causes

https://doi.org/10.1021/acsomega.4c01993
ACS Omega 2024, 9, 21484−21493

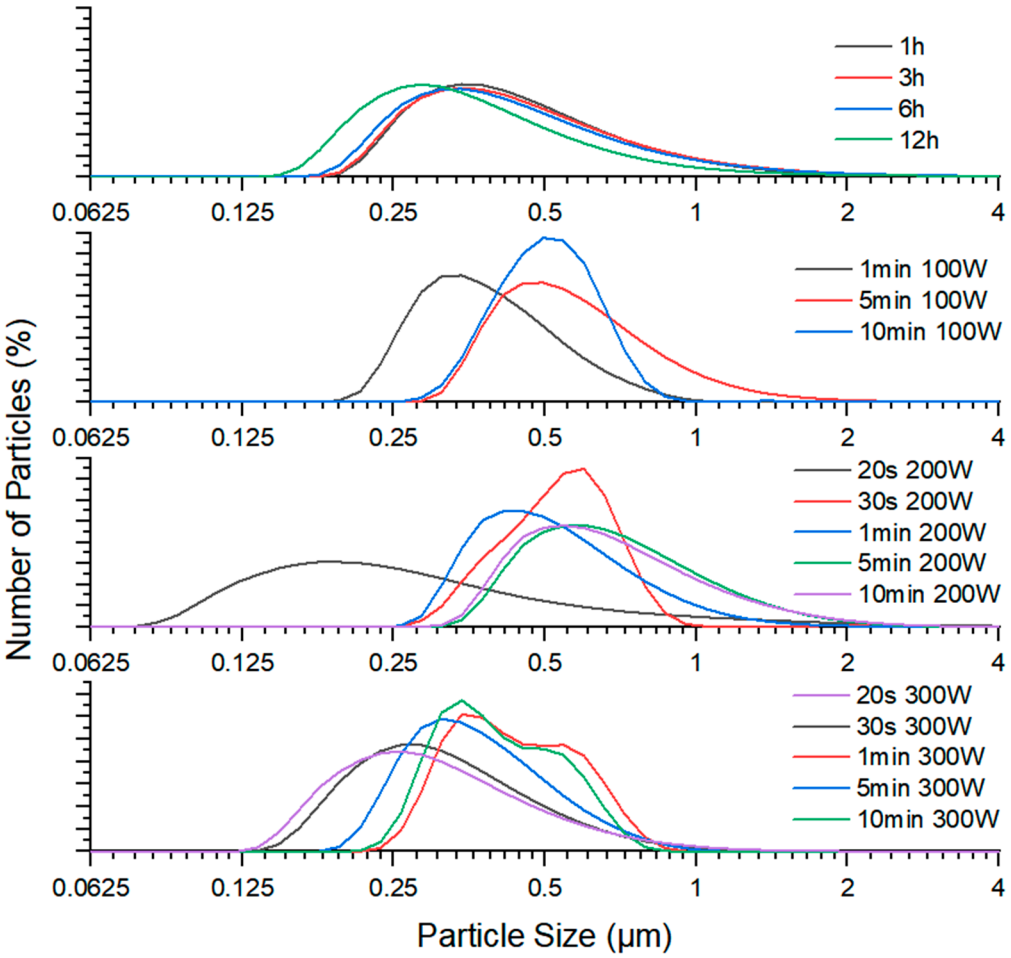

Figure 9. Particle size distribution graphs of FeTHQ synthesized under various conditions. The first graph indicates the solvothermal-synthesized FeTHQ in different times, and the subsequent graphs are the results of microwave-synthesized FeTHQ at varying times and power conditions.

agglomeration between the FeTHQ particles[20] and leads to the detection of larger particles (Figure 11).

4. CONCLUSION

Ellagic acid-based SU-101, THQ-based FeTHQ, and HHTP-based Cu-CAT-1 were studied as effective antioxidants. Considering the three criteria for an effective antioxidant, optimal particle size, biocompatibility, and long-term effects, FeTHQ proved to be an eligible antioxidant. FeTHQ released an average of 332 ORAC units of antioxidant capacity every 12 h interval, which surpasses the antioxidative capability of common vegetables.[21]

To discover the conditions for synthesizing FeTHQ with optimal particle size, we conducted microwave-assisted methods with different time and power conditions and compared them with conventional solvothermal methods. As a result, the solvothermal-synthesized FeTHQ had a broader size distribution but a smaller mode. In contrast, the microwave-synthesized MOFs had a narrower distribution, and 300 W conditions yielded the smallest crystals. Considering the proportion of small crystals (<1 μm), along with the PXRD and IR results, we concluded that 1 min at 300 W was the optimal condition for yielding the most "usable" crystals: particles with adequate size to be absorbed in the body without being excreted.

However, the introduction of particles over 200 nm in size into Kupffer cells and the potential subsequent lysosomal degradation presents a complexity that warrants further investigation.[22] The acidic environment of lysosomes may affect the stability of FeTHQ and its antioxidant production, thereby potentially having adverse effects on the cells. In that sense, *in vitro* biocompatibility tests using Kupffer cells should be conducted, as well as analysis of MOF stability in the lysosomal environment to ensure not only the efficacy but also the safety of FeTHQ as an antioxidant.

Nevertheless, the promising results of FeTHQ encourage further exploration into its applications in the medical and nutritional fields, which emphasizes the need for comprehensive studies on its intake pathways and interactions within biological systems. Future studies should aim to address these concerns to pave the way for the development of safe and effective long-term antioxidant therapies.

■ ASSOCIATED CONTENT

Supporting Information

The Supporting Information is available free of charge at https://pubs.acs.org/doi/10.1021/acsomega.4c01993.

Particle size distribution data, specific ORAC values, PXRD data, IR spectra, and TGA data (PDF)

https://doi.org/10.1021/acsomega.4c01993
ACS Omega 2024, 9, 21484−21493

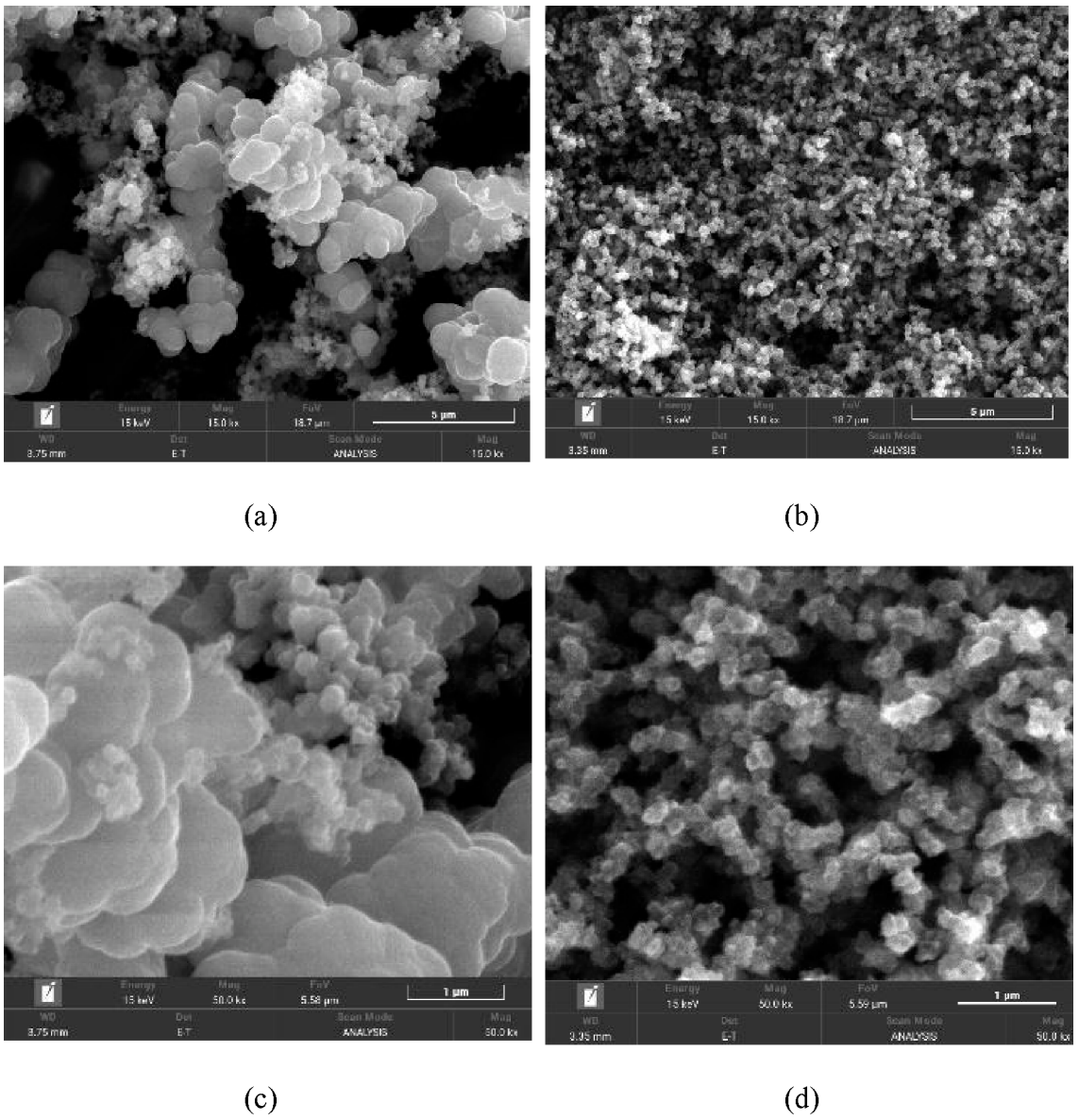

Figure 10. SEM image of (a) solvothermal FeTHQ, 15 000×; (b) microwave FeTHQ, 15 000×; (c) solvothermal FeTHQ, 50 000×; and (d) microwave FeTHQ, 50 000×.

AUTHOR INFORMATION

Corresponding Author

Eun-Young Choi − *Korea Science Academy of KAIST, Busan 47162, Republic of Korea; Department of Chemistry, Korea Advanced Institute of Science and Technology (KAIST), Daejeon 34141, Republic of Korea;* orcid.org/0000-0002-6224-8664; Email: faujasite1@kaist.ac.kr

Authors

Woojin Park − *Korea Science Academy of KAIST, Busan 47162, Republic of Korea; Department of Chemistry, Korea Advanced Institute of Science and Technology (KAIST), Daejeon 34141, Republic of Korea;* orcid.org/0009-0002-5929-4624

Sanghyun Park − *Korea Science Academy of KAIST, Busan 47162, Republic of Korea; Department of Biological Sciences, Korea Advanced Institute of Science and Technology (KAIST), Daejeon 34141, Republic of Korea*

Ki-Youb Park − *Korea Science Academy of KAIST, Busan 47162, Republic of Korea*

Complete contact information is available at: https://pubs.acs.org/10.1021/acsomega.4c01993

Author Contributions

W.P. and S.P. conceived the study. E.-Y.C. supervised the research. W.P. played a leading role in experimentations. S.P. performed experiments related to particle size distribution analysis. K.-Y.P. played a supportive role in biology experimentations. E.-Y.C., W.P., and S.P. wrote the paper.

Notes

The authors declare no competing financial interest.

ACKNOWLEDGMENTS

This work was supported by the Korea Science Academy of KAIST with funds from the Ministry of Science and ICT in

https://doi.org/10.1021/acsomega.4c01993
ACS Omega 2024, 9, 21484−21493

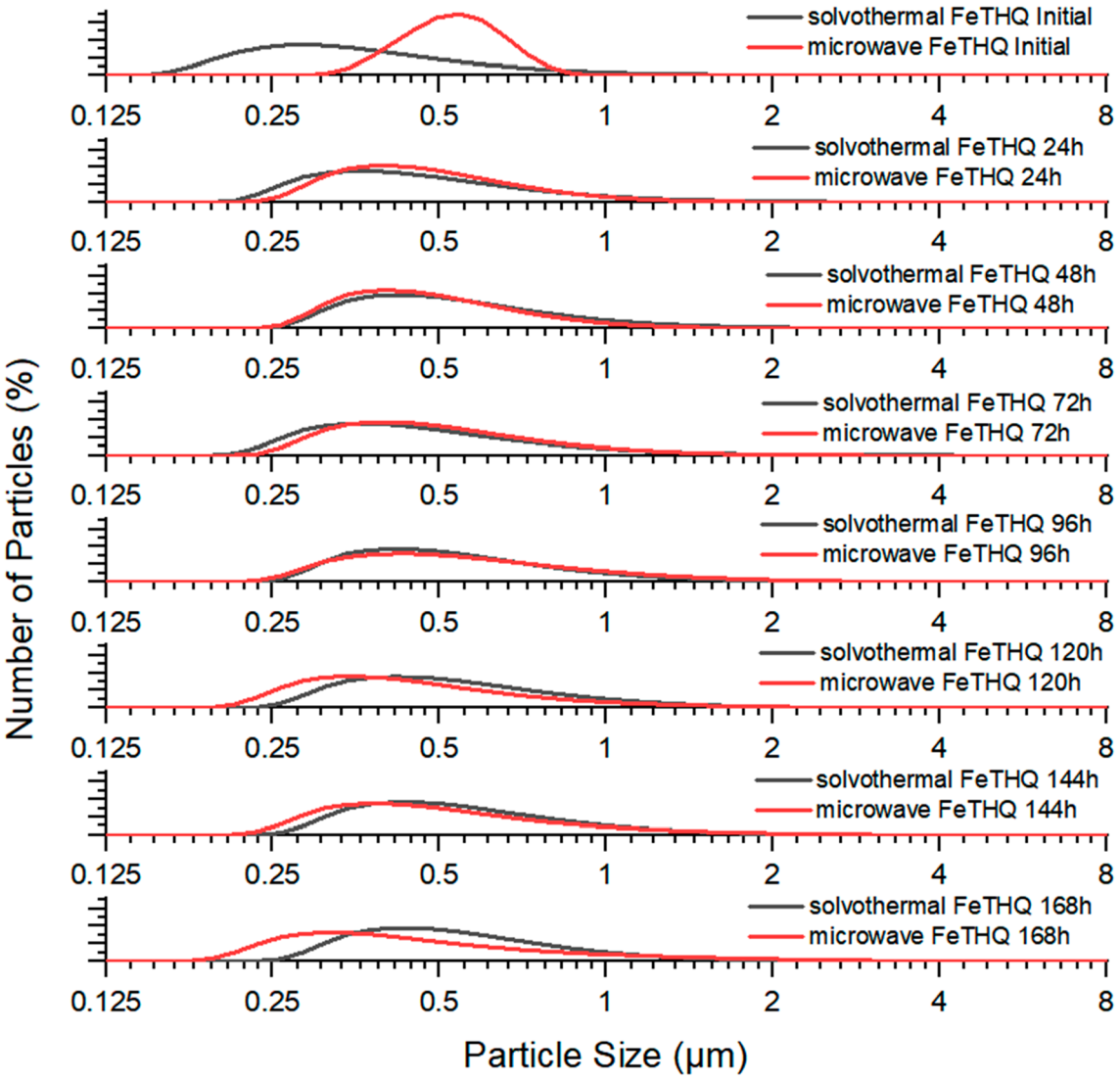

Figure 11. Particle size distribution change of solvothermal-synthesized FeTHQ and microwave-synthesized FeTHQ over 7 days.

Korea. Neuronal stem cells were provided by Professor Man Su Kim (Ph.D., Inje University).

REFERENCES

(1) Zhang, Y.-J.; Gan, R.-Y.; Li, S.; Zhou, Y.; Li, A.-N.; Xu, D.-P.; Li, H.-B. Antioxidant phytochemicals for the prevention and treatment of chronic diseases. *Molecules* **2015**, *20* (12), 21138−21156.

(2) Eddaoudi, M.; Moler, D. B.; Li, H.; Chen, B.; Reineke, T. M.; O'Keeffe, M.; Yaghi, O. M. Modular chemistry: secondary building units as a basis for the design of highly porous and robust metal-organic carboxylate frameworks. *Acc. Chem. Res.* **2001**, *34* (4), 319−330.

(3) Liu, D.; Zou, D.; Zhu, H.; Zhang, J. Mesoporous metal-organic frameworks: synthetic strategies and emerging applications. *Small* **2018**, *14* (37), 1801454.

(4) El-Bindary, M. A.; El-Desouky, M. G.; El-Bindary, A. A. Metal-organic frameworks encapsulated with an anticancer compound as drug delivery system: Synthesis, characterization, antioxidant, anticancer, antibacterial, and molecular docking investigation. *Appl. Organomet. Chem.* **2022**, *36* (5), No. e6660.

(5) Cooper, L.; Hidalgo, T.; Gorman, M.; Lozano-Fernández, T.; Simón-Vázquez, R.; Olivier, C.; Guillou, N.; Serre, C.; Martineau, C.; Taulelle, F.; et al. A biocompatible porous Mg-gallate metal-organic framework as an antioxidant carrier. *Chem. Commun.* **2015**, *51* (27), 5848−5851.

(6) MatthiasGolomb. MatthiasGolomb/CuHHTP_EDL: Working repository. *Zenodo* 2021. DOI: 10.5281/zenodo.4694845.

(7) Groom, C. R.; Bruno, I. J.; Lightfoot, M. P.; Ward, S. C. The Cambridge structural database. *Acta Crystallographica Section B: Structural Science, Crystal Engineering and Materials* **2016**, *72* (2), 171−179.

(8) Egorova, K. S.; Ananikov, V. P. Toxicity of metal compounds: knowledge and myths. *Organometallics* **2017**, *36* (21), 4071−4090.

(9) Grape, E. S.; Flores, J. G.; Hidalgo, T.; Martínez-Ahumada, E.; Gutiérrez-Alejandre, A.; Hautier, A.; Williams, D. R.; O'Keeffe, M.; Öhrström, L.; Willhammar, T.; et al. A robust and biocompatible bismuth ellagate MOF synthesized under green ambient conditions. *J. Am. Chem. Soc.* **2020**, *142* (39), 16795−16804.

(10) Chen, G.; Gee, L. B.; Xu, W.; Zhu, Y.; Lezama-Pacheco, J. S.; Huang, Z.; Li, Z.; Babicz, J. T., Jr; Choudhury, S.; Chang, T.-H.; et al. Valence-Dependent Electrical Conductivity in a 3D Tetrahydroxyquinone-Based Metal-Organic Framework. *J. Am. Chem. Soc.* **2020**, *142* (51), 21243−21248.

(11) Hmadeh, M.; Lu, Z.; Liu, Z.; Gándara, F.; Furukawa, H.; Wan, S.; Augustyn, V.; Chang, R.; Liao, L.; Zhou, F.; et al. New porous crystals of extended metal-catecholates. *Chem. Mater.* **2012**, *24* (18), 3511−3513.

(12) Ni, Z.; Masel, R. I. Rapid production of metal- organic frameworks via microwave-assisted solvothermal synthesis. *J. Am. Chem. Soc.* **2006**, *128* (38), 12394−12395.

https://doi.org/10.1021/acsomega.4c01993
ACS Omega 2024, 9, 21484−21493

(13) Park, K.-Y.; Na, Y.; Kim, M. S. Role of nox4 in neuronal differentiation of mouse subventricular zone neural stem cells. *Journal of Life Science* **2016**, *26* (1), 8−16.
(14) Schneider, C. A.; Rasband, W. S.; Eliceiri, K. W. NIH Image to ImageJ: 25 years of image analysis. *Nat. Methods* **2012**, *9* (7), 671−675.
(15) Huang, D.; Ou, B.; Prior, R. L. The chemistry behind antioxidant capacity assays. *Journal of agricultural and food chemistry* **2005**, *53* (6), 1841−1856.
(16) Re, R.; Pellegrini, N.; Proteggente, A.; Pannala, A.; Yang, M.; Rice-Evans, C. Antioxidant activity applying an improved ABTS radical cation decolorization assay. *Free Radical Biol. Med.* **1999**, *26* (9), 1231−1237.
(17) Hirschle, P.; Preiß, T.; Auras, F.; Pick, A.; Völkner, J.; Valdepérez, D.; Witte, G.; Parak, W. J.; Rädler, J. O.; Wuttke, S. Exploration of MOF nanoparticle sizes using various physical characterization methods-is what you measure what you get? *CrystEngComm* **2016**, *18* (23), 4359−4368.
(18) Hu, J.; Chen, Y.; Zhang, H.; Chen, Z. Controlled syntheses of Mg-MOF-74 nanorods for drug delivery. *J. Solid State Chem.* **2021**, *294*, 121853.
(19) Reineke, J. J.; et al. Unique insights into the intestinal absorption, transit, and subsequent biodistribution of polymer-derived microspheres. *Proc. Natl. Acad. Sci. U. S. A.* **2013**, *110* (34), 13803−13808.
(20) Caballero-Díaz, E.; Pfeiffer, C.; Kastl, L.; Rivera-Gil, P.; Simonet, B.; Valcárcel, M.; Jiménez-Lamana, J.; Laborda, F.; Parak, W. J. The toxicity of silver nanoparticles depends on their uptake by cells and thus on their surface chemistry. *Particle & Particle Systems Characterization* **2013**, *30* (12), 1079−1085.
(21) Ou, B.; Huang, D.; Hampsch-Woodill, M.; Flanagan, J. A.; Deemer, E. K. Analysis of antioxidant activities of common vegetables employing oxygen radical absorbance capacity (ORAC) and ferric reducing antioxidant power (FRAP) assays: a comparative study. *J. Agric. Food Chem.* **2002**, *50* (11), 3122−3128.
(22) Blanco, E.; Shen, H.; Ferrari, M. Principles of nanoparticle design for overcoming biological barriers to drug delivery. *Nature biotechnology* **2015**, *33* (9), 941−951.

https://doi.org/10.1021/acsomega.4c01993
ACS Omega 2024, 9, 21484−21493